ÓPTICA PURA Y APLICADA
www.sedoptica.es

Type: RESEARCH PAPER
Section: DO NOT WRITE HERE

Optical and neural contribution on the visual function in mesopic and photopic adaptations

Contribución óptica y neural en la función visual en adaptación mesópica y fotópica

R. Sánchez[1*], L. Calderari[1], L. Issolio[1,2]

1. Instituto de Investigación en Luz, Ambiente y Visión (ILAV), Tucumán, Argentina

2. Universidad Nacional de Tucumán (UNT), Tucumán, Argentina

(*) E-mail: rsanchez@herrera.unt.edu.ar S: miembro de SEDOPTICA / SEDOPTICA member

Received: 29/03/2023 Accepted: 25/06/2023
DOI: 10.7149/OPA.56.2.51139

ABSTRACT:

We study the relative contribution of optical and neural factors on contrast sensitivity for mesopic to photopic lighting. MTFs were determined from double-pass images on a group of seven young normal vision subjects and the calculation of the neural transfer function (NTF) was performed by mean of a model that includes the photon noise, the neural noise and the lateral inhibition. In order to analyze the changes in visual sensitivity resulting from lighting, the areas under the curves (AUC) of both the MTFs, NTFs and CSFs were computed for seven lighting levels (0.005, 0.025, 0.5, 5, 35, 320, and 950 cd/m^2). Besides, Strehl ratio, MTF cut-off frequency and CSF cut-off frequency were determined. The NTFAUC as a function of luminance shown the steepest slope in the mesopic range and then flattening towards the maximum measured luminance for the photopic range, while the MTFAUC shows small variations in the mesopic and undergoes a sustained increase in the photopic. The variation of MTF and CSF cut-off frequencies shown that, for the mesopic range, the MTF cut-off frequencies are above to the CSF cut-off frequencies suggesting the optical response is limited by the neural processing but, in the photopic range, both curves continue to grow reaching a coincident response suggesting the neural response account for the high spatial resolution provides by the optics of the eye.

Key words: light adaptation, contrast sensitivity, optical quality

RESUMEN:

Se estudia la contribución relativa de los factores ópticos y neurales en la sensibilidad al contraste para iluminación mesópica y fotópica. Las MTFs se determinaron a partir de imágenes de doble paso en un grupo de siete sujetos jóvenes con visión normal y el cálculo de la función de transferencia neural (NTF) se realizó mediante un modelo que incluye el ruido fotónico, el ruido neural y la inhibición lateral. Para analizar los cambios en la sensibilidad visual debidos a la iluminación, se calcularon las áreas bajo las curvas (AUC) de MTF, NTF y FSC para siete niveles de iluminación (0,005, 0,025, 0,5, 5, 35, 320 y 950 cd/m^2). Además, se determinaron las relaciones de Strehl, las frecuencias de corte de la MTF y de la FSC. La NTFAUC en función de la luminancia muestra una pendiente pronunciada en el rango mesópico y luego se aplana hacia la luminancia máxima medida en el rango fotópico, mientras que el MTFAUC muestra pequeñas variaciones en el mesópico y experimenta un aumento sostenido en el fotópico. En el rango mesópico, las frecuencias de corte de las MTF están por encima de las frecuencias de corte de CSF, sugiriendo que la respuesta óptica está limitada por el procesamiento neural, aunque en el rango fotópico ambas curvas siguen creciendo hasta alcanzar una respuesta coincidente que indicaría que en ese rango la respuesta neuronal da cuenta de la alta resolución espacial proporcionada por la óptica del ojo.

Palabras clave: adaptación a la luz, sensibilidad al contraste, calidad óptica

REFERENCES AND LINKS / REFERENCIAS Y ENLACES

[1] A. Stockman, L. T. Sharpe, "Into the twilight zone: the complexities of mesopic vision and luminous efficiency," Ophthalmic Physiol Opt. **26**(III), 225-239 (2006).

[2] W. A. Rushton, G. H. Henry, "Bleaching and regeneration of cone pigments in man," Vision Res. **8**(VI), 617-631 (1968).

[3] F. Díaz-Doutón, A. Benito, J. Pujol, M. Arjona, J. L. Güell, P. Artal, "Comparison of the retinal image quality with a Hartmann-Shack wavefront sensor and a double-pass instrument," Invest Ophthalmol Vis Sci. **47**(IV), 1710-1716 (2006).

[4] P. Barrionuevo, E. Colombo, D. Corregidor, M. Jaén, L. Issolio, "Evaluation of the intraocular diffusion through brightness reduction by glare using ectopic diffusers to simulate cataracts," Optica Applicata **40**(I), 63-75 (2010).

[5] J. Santamaría, P. Artal, J. Bescós, "Determination of the point-spread function of human eyes using a hybrid optical-digital method," J Opt Soc Am A. **4**(VI), 1109-1114 (1987).

[6] P. Artal, "Image formation in the living human eye," Annu Rev Vis Sci. **24**(I), 1-17 (2015).

[7] R. Shapley, C. Enroth-Cugell, "Chapter 9 Visual adaptation and retinal gain controls," Progress in Retinal Research **3**, 263-346 (1984).

[8] J. L. Gardner, E. P. Merriam, J. A. Movshon, D. J. Heeger, "Maps of visual space in human occipital cortex are retinotopic, not spatiotopic," J Neurosci. **28**(XV), 3988-3999 (2008).

[9] D. B. Elliott, "Contrast sensitivity decline with ageing: a neural or optical phenomenon?," Ophthalmic Physiol Opt. **7**(IV), 415-419 (1987).

[10] M. E. Sloane, C. Owsley, C. A. Jackson, "Aging and luminance-adaptation effects on spatial contrast sensitivity," J Opt Soc Am A. **5**(XII), 2181-2190 (1988).

[11] M. E. Sloane, C. Owsley, S. L. Alvarez, "Aging, senile miosis and spatial contrast sensitivity at low luminance," Vision Res. **28**(XI), 1235-1246 (1988).

[12] D. Elliott, D. Whitaker, D. MacVeigh, "Neural contribution to spatiotemporal contrast sensitivity decline in healthy ageing eyes," Vision Res. **30**(IV), 541-547 (1990).

[13] K. B. Burton, C. Owsley, M. E. Sloane, "Aging and neural spatial contrast sensitivity: photopic vision," Vision Res. **33**(VII), 939-946 (1993).

[14] S. Pardhan, J. Gilchrist, D. B. Elliott, G. K. Beh, "A comparison of sampling efficiency and internal noise level in young and old subjects," Vision Res. **36**(XI), 1641-1648 (1996).

[15] G. D. Hastings, J. D. Marsack, L. N. Thibos, R. A. Applegate, "Combining optical and neural components in physiological visual image quality metrics as functions of luminance and age," J Vis. **20**(VII), 1-20 (2020).

[16] R. F. Sánchez, C. E. García-Guerra, J. A. Martínez-Roda, A. G. de Paul, L. A. Issolio, J. Pujol, "Implementation of the frequency scatter index in clinical commercially available double-pass systems," Curr Eye Res. **47**(III), 391-398 (2022).

[17] P. Artal, I. Iglesias, N. López-Gil, D. G. Green, "Double-pass measurements of the retinal-image quality with unequal entrance and exit pupil sizes and the reversibility of the eye's optical system," J Opt Soc Am A Opt Image Sci Vis. **12**(X), 2358-2366 (1995).

[18] J. A. Martínez-Roda, M. Vilaseca, J. C. Ondategui, M. Aguirre M, J. Pujol, "Effects of aging on optical quality and visual function," Clin Exp Optom. **99**(VI), 518-525 (2016).

[19] P. G. J. Barten, "Contrast sensitivity of the human eye and its effects on image quality," Institute for Perception Research, Eindhoven (1999).

[20] F. W. Campbell, D. G. Green, "Optical and retinal factors affecting visual resolution," J Physiol. **181**(III), 576-593 (1965).

[21] W. S. Stiles, B. H. Crawford, "The luminous efficiency of rays entering the eye pupil at different points," Proceedings of the Royal Society (London) B **112**, 428-450 (1933).

[22] N. López-Gil, P. Artal, "Comparison of double-pass estimates of the retinal image quality obtained with green and near infrared light," J. Opt. Soc. Am. A **14**(V), 961-971 (1997).

[23] J. A. Martínez-Roda, C. E. García-Guerra, F. Diaz-Doutón, J. Pujol, A. Salvador, M. Vilaseca, "Quantification of forward scattering based on the analysis of double-pass images in the frequency domain," Acta Ophthalmol. **97**(VII), 1019-1026 (2019).

[24] K. Purpura, E. Kaplan, R. M. Shapley, "Background light and the contrast gain of primate P and M retinal ganglion cells," Proc Natl Acad Sci USA **85**(XII), 4534-4537 (1988).

[25] D. Cao, B. B. Lee, H. Sun, "Combination of rod and cone inputs in parasol ganglion cells of the magnocellular pathway," J Vis. **10**(XI), 1-22 (2010).

[26] F. L. van Nes, J. J. Koenderink, H. Nas, M. A. Bouman, "Spatiotemporal modulation transfer in the human eye," J Opt Soc Am. **57**(IX), 1082-1088 (1967).

[27] J. Rovamo, J. Mustonen, R. Näsänen, "Modelling contrast sensitivity as a function of retinal illuminance and grating area," Vision Res. **34**(X), 1301-1314 (1994).

[28] R. Xu, H. Wang, L. N. Thibos, A. Bradley, "Interaction of aberrations, diffraction, and quantal fluctuations determine the impact of pupil size on visual quality," J Opt Soc Am A Opt Image Sci Vis. **34**(IV), 481-492 (2017).

[29] A. Watson, A. Ahumada, "Predicting visual acuity from wavefront aberrations," J Vis. **8**(IV), 17,1-19 (2008).

[30] D. A. Atchison, G. Smith, N. Efron, "The effect of pupil size on visual acuity in uncorrected and corrected myopia," Am J Optom Physiolog Opt. **56**(V), 315–323 (1979).

[31] T. T. Berendschot, P. J. DeLint, D. van Norren, "Fundus reflectance-historical and present ideas," Prog Retin Eye Res. **22**(II), 171-200 (2003).

1. Introduction

Light adaptation in the human visual system is an important capacity that allows people to detect and process stimulation from the lighting environment in a particularly large range that spans more than 10 log units [1]. Several dynamic mechanisms exist to obtain the maximal response at each lighting level, the most notable being the cone-rod photoreceptor duality, which splits the visual response range into three stages: the scotopic dominated by the rods, the photopic dominated by the cones, and the mesopic, the intermediate range characterized by the simultaneous response of both photoreceptors. On the other hand, the photoreceptors reach more or less stable levels of adaptation through the concentration of their photopigments with a slow response to changes in lighting [2]. Following the visual pathway, photoreceptors and postreceptoral retinal cells (horizontal, bipolar, and amacrine cells) constitute the substrate where gain control mechanisms are produced, responsible for fast adaptation processes. On the other hand, the variation of the pupil diameter works throughout the entire range of adaptation, regulating only a small amount of light of barely more than a log unit. However, its most important role is to control aberrations that produce dramatic changes in image quality on the retina. Throughout this range of light adaptation, both the optical system and the neural response of the cells of the retina and the brain have modifications in order to achieve an optimal response of the visual system.

The optical quality of the eye is largely determined by optical aberrations, scattering and, only for very small pupils, by diffraction [3]. In the scattering, part of the light that enters the eye is deviated from its trajectory due to the presence of inhomogeneities in the ocular media that the light passes through. These light beams deflected from their original direction produce a veil of light that reduces retinal contrast and decreasing image quality on the retina [4]. On the other hand, in a real optical system, aberrations produce a wavefront that is not completely spherical avoiding optimal focusing of the light beams. As a result, the combined effect of scattering and aberrations affect the visual quality of the eye and, together with the smaller sizes of the photoreceptors, impose a limit on the visual system resolution.

The retinal image quality can be assessed by recording double-pass images, from which the point spread function (PSF) is obtained, describing the way in which light from a point source is spatially distributed [5]. The response of the optics of the eye to different spatial frequencies, i.e., the modulation transfer function (MTF) can be computed by the Fourier transform of the double-pass image. To measure the aberrations, the difference between the wavefront generated by the eye and a reference wavefront is quantified, obtaining the wave aberration function which describes both refractive errors and high order aberrations and depends on the pupil diameter [6]. Both methods allow characterizing the quality of the retinal image.

In addition to optical factors, visual sensitivity is determined by factors typical of neural processing. Photon noise is the fluctuation in the number of photons exciting photoreceptors at the stage of signal transduction, affecting the detection threshold at low luminance levels; neural noise, caused by statistical fluctuations in

the signal transported to the brain through a group of nerve fibers and, the contrast gain, a nonlinear negative feedback that is present in different cells of the retina [7] as well as in the visual cortex [8]. These neural mechanisms combined with the MTF describe the global spatial response of the visual system, the contrast sensitivity function (CSF).

The way in which optical and neural factors contribute to the adaptation process has been extensively studied, although most of these works were aimed at studying the contribution of these factors to changes with age suggesting that the neural system plays a major role in the loss of contrast sensitivity with aging in normal eyes [9-14]. Hastings *et al.* have recently made a fairly comprehensive description about the roles and interactions of optical and neural components in foveal visual image quality as function of the target luminance but also considering the age effects in a wide range [15].

In the present work we study the relative contribution of optical and neural effects on contrast sensitivity for different lighting levels ranging from mesopic to photopic levels. The proposal is based on MTF measurements performed on a group of young subjects with normal vision, with the idea of later incorporating an age-dependent visual response model. The MTF is determined from double-pass images which present the degradation of both ocular aberrations and intraocular scattering. Besides, we compute the neural transfer function (NTF) by mean of a model that includes the photon noise, the neural noise and the effect of the lateral inhibition and, which has also shown to be a suitable tool for this purpose and accounting for a variety of CSF results obtained in very different conditions.

2. Methods

2.a. Experimental setup

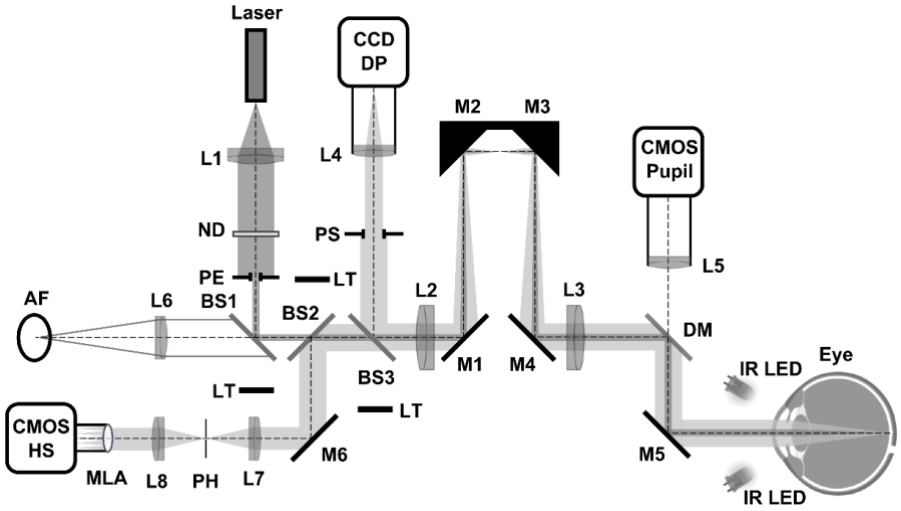

Fig.1. Layout of the experimental setup to analyze the optical quality of the eye in different lighting conditions. PE, entrance pupil; PS, exit pupil; BS, beam splitter; L, lens; M, mirror; Laser, laser diode; CCD, CCD camera; CMOS, CMOS camera; MLA, microlens array; DM, dichroic mirror; ND, neutral filter; AF, adaptation field; PH, pinhole; LT, light trap; IR LED, Infrared light-emitting diode. In dark grey, the optical path of the first pass; in light grey, the optical path of the second pass.

The experimental setup, shown in Fig. 1, is slightly modified from that used in previous experiments and described in detail elsewhere [16]. Briefly, a filtered infrared laser diode (MC7850CPWR-SMF, wavelength 785 nm) coupled to an optical fiber was used as a point source. Light coming from the output of the optical fiber is collimated (aspheric lens, L1) and passes through the aperture PE (2 mm), which acts as the stop for the first pass. The light is reflected by the beam splitter (BS1), passes through an achromatic Badal system (lenses L2, L3, mirrors M1, M2, M3, and M4) before reaching the eye. A CMOS camera (UI-1221LE-M-GL, IDS Imaging Development Systems GmbH, Germany) monitors the eye pupil through a long-pass dichroic mirror (DM, 850 nm cut-on wavelength) when the eye is illuminated with 900 nm LEDs. This allows the alignment of the eye pupil along the optical axis of the measuring setup and correlate the pupil size with the optical quality parameters measured with both sensors (Hartmann-Shack and double-pass). The light coming from the point source and reflected in the retina passes through lenses L2, L3, and the aperture diaphragm PS (stop of the second pass when the natural pupil is bigger than the aperture), forming the double-pass image, which is collected by a CCD camera (UI-2220ME-M, IDS Imaging Development Systems

GmbH, Germany). The light transmitted by BS3 is then reflected by BS2 and sampled by the microlens array (MLA, 0200-6.3-S-C, square geometry, 6.3 mm focal length, single microlens aperture of 200 μm). A CMOS camera (UI-1120SE-M-GL, IDS Imaging Development Systems GmbH, Germany), CMOS HS, placed at the focus location of the MLA records Hartmann-Shack images. An adaptation field located at optical infinity by lens L6 (f=35 mm) is used to achieve seven different levels of illumination: 0.005, 0.025, 0.5, 5, 35, 320, and 950 cd/m^2. This field consists of a circular diffuser screen, concentric with the optical axis of the system, uniformly backlit by a high-power white LED plus a collimation lens. To achieve the different lighting levels, the LED is powered by a specifically developed driver. The luminance of the adaptation field was measured at the exit of the system in the pupil plane with a luminance meter (LMT L1009, LMT Lichtmesstechnik GmbH, Germany).

2.b. Subjects

Seven young healthy volunteers with a mean age of 33 years old were considered for the measurements. The inclusion criteria were corrected distance visual acuity of 20/20 or higher, spherical refraction in the range of -1.5 to +1.5 D, astigmatism less than -1.0 D, pupil diameter of 4 mm or greater under photopic conditions and absence of a history of ocular diseases, surgery or pharmacological treatment. Ethical approval for this study was obtained from the Research Ethics Committee (CEI) of the Universidad Nacional de Tucumán and Consejo Nacional de Investigaciones Científicas y Técnicas. Every volunteer was informed about the topics of the study, and a written informed consent was obtained, following the tenets of the Declaration of Helsinki.

2.c. Experimental procedure

To analyse the impact of the aberrations in different lighting levels, Hartmann-Shack and double-pass measurements were performed in the subjects with three mesopic levels (0.005, 0.025, and 0.5 cd/m^2) and four photopic levels (5, 35, 320, and 950 cd/m^2). The measurements were taken after the subject was adapted to each level in a dark room for ten minutes to obtain a naturally dilated pupil, from the lower level to the higher one. The aperture diaphragm PS was set at its maximum opening (15 mm) so the effective exit pupil of the system corresponded to the natural pupil of the subject adapted to any of the established lighting levels. In each record, six double-pass images, six Hartmann-Shack images, and the pupil image were simultaneously taken per subject after correcting spherical refractive errors with the Badal system of the instrument. During the acquisition time, the position of the pupil of the subject was monitored. Because centring the pupil with respect to the optical axis of the system is fundamental to avoid introducing errors in the measurement, whenever a movement was observed during the acquisition, the data were discarded and the measurement for that condition was repeated. Between each condition, the subject was asked to blink naturally, avoiding the visualization of another light source.

2.d. Data processing

A MATLAB script was used for the calculation of the pupil diameter from the images of the pupil camera. Previously, a pattern with a scale in tenths of a millimeter was measured in the pupil plane to calibrate the images of the pupil camera. Hartmann-Shak images were processed by a MATLAB script to obtain the corresponding Zernike coefficients. The root mean square wavefront error (RMS) was computed from the Zernike coefficients and was used as indicators of the residual low and high order aberrations of the measured eye introduced by the variations in the pupil size due to a luminance change. In all the cases, the image used for the analysis was obtained by averaging the six available frames per measurement and the subsequent subtraction of the corresponding background image. Double-pass images were processed by an ImageJ script to obtain the MTF curve. From each set of six double-pass images, an average image was computed and then the background was subtracted from this average. Then, a cropped version of this double-pass image (256x256 pixels) was used for the analysis. The MTF was computed by dividing the modulus of the Fourier transform of the double-pass image by the diffraction-limited MTF [17]. From this two-dimensional MTF, one-dimensional MTF profile was obtained by averaging across all directions. The cut-off frequency of MTF curve (MTF cut-off) was estimated as that corresponding to a value of 0.01, since the profile computed from the real double-pass image background has noise [18]. The Strehl ratio (SR) was computed as the relation between the areas under the mean MTFs curves of the measured eyes and that of

the aberration-free eye. In addition, the frequency scatter index (FSI) was calculated for each condition to evaluate the effect of intraocular scattering [16].

Neural transfer function (NTF) curves were computed with the Barten's model including the action of the photon noise, neural noise, and the contrast gain [19]. For the calculation of the NTFs, the luminance values used in the MTF measurements were employed, as well as the values of the mean pupil diameter measured in each of these lighting levels, so that the model is truly representative of the experimental conditions. Contrast sensitivity function (CSF) curves were obtained by the convolution between the MTF and the NTF curves [20]. The cut-off frequency of the CSF curve (CSF cut-off) was estimated as a value of 1 which corresponds to a threshold contrast of 100 %. In order to compare the different functions with each other (MTF, NTF, and CSF) the areas under the curves (AUC) were computed.

3. Results

Table 1 presents the mean pupil diameter (PD) of the 7 subjects for each luminance level of the adaptation field (L) used for the MTF measurement, and the retinal illuminance computed from L, PD and corrected for the Stiles and Crawford effect [19,

21].

TABLE 1. Luminance of the adaptation field, mean pupil diameter, and the computed retinal illuminance.

Luminance [cd/m^2]	Pupil diameter [mm]	Eret [td]
0.005	6.2	0.1
0.025	6.1	0.5
0.5	5.6	9
5	4.9	73
35	4.4	430
320	3.8	3100
950	3.5	8000

Mean MTF curves obtained from seven subjects to the seven lighting levels studied are shown in Fig. 2. The curves were normalized and corrected to a visible wavelength of 555 nm [22]. The curves corresponding to the photopic range (blue curves) are ordered ascending with the luminance while those obtained in the mesopic range (black curves) intersect each other without following the ascending order of luminance.

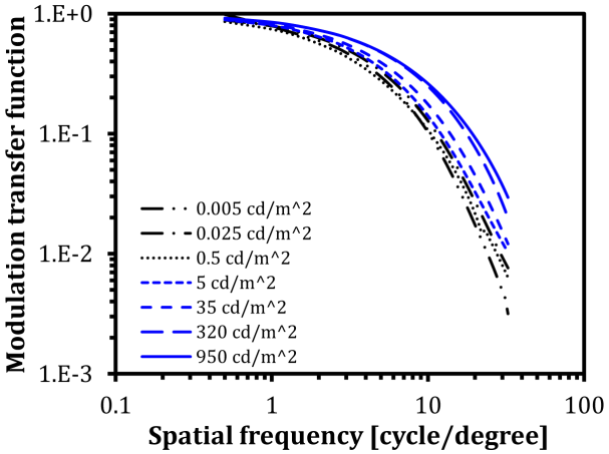

Fig. 2. Mean MTFs determined for seven young subjects and seven luminance levels. Black curves correspond to mesopic levels, while blue curves at photopic levels.

Table 2 shows the average values for the seven subjects at each luminance condition of the different optical quality parameters obtained both from double-pass measures (SR and MTF cut-off) and from wavefront aberrations measures (RMS), along with other visual quality parameters (CSF cut-off and VA). As it can be seen, the SR increases while the RMS decreases when the lighting level of the adaptation field increases, both behaviours are consequence of a decrease in the pupil size. Also, as expected, the MTF cut-off value

was increased with the same trend presented by the SR. The SR obtained for 35 cd/m² is 0.231 and the value obtained for others authors at the same luminance is slightly higher (0.265) because these authors used a commercial optical quality measurement system with a fixed exit pupil of 4 mm, a little less than the 4.4 mm of our measurements [18]. In order to complete the analysis of the MTF, and to evaluate the effects of scattering in the MTF measured, we determine the frequency scatter index (FSI) for all the subjects and luminance levels, obtaining a mean value of 0.43 ± 0.02 similar to that obtained previously in a young population for the same range of pupil sizes [16,23].

TABLE 2. Mean RMS wavefront error, mean Strehl ratio, MTF and CSF cut-off frequencies, and the estimated visual acuity for the luminance range used in the experiment.

Luminance [cd/m²]	RMS [μm]	Strehl ratio	MTF cut-off [cycle/degree]	CSF cut-off [cycle/degree]	VA
0.005	0.162	0.175	24.0	8.0	0.3
0.025	0.145	0.200	29.0	11.0	0.4
0.5	0.140	0.169	27.5	16.0	0.5
5	0.088	0.204	33.0	24.5	0.8
35	0.092	0.231	34.5	32.0	1.1
320	0.065	0.282	38.0	38.0	1.3
950	0.078	0.300	43.0	43.0	1.4

Fig. 3 shows the neural transfer function (NTF) curves that represent the response of the retina-brain system calculated with the Barten's model including the action of the photon noise, neural noise and the lateral inhibition [19]. The computed NTFs curves clearly show how neural processing is also strongly affected by the lighting level, increasing sensitivity to illumination [24,25].

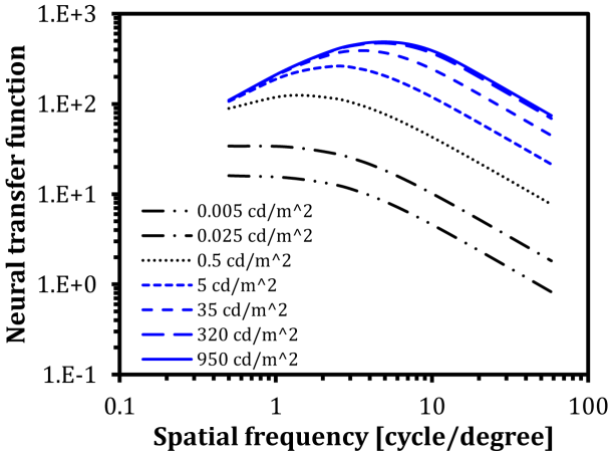

Fig. 3. NTFs for seven luminance levels computed from the Barten's model [19]. Black curves correspond to mesopic levels, while blue curves at photopic levels.

Fig. 4 shows the contrast sensitivity function (CSF) curves for the seven lighting levels obtained by the convolution between the measured MTFs and the computed NTFs curves [20], that express the global spatial response of the visual system. The CSFs curves obtained show the typical growth as a function of illumination [26] that synthesizes the improvement in visual quality due to the decrease in aberrations and the increase in sensitivity of the retina-brain system due to the action of the known mechanisms of contrast gain. Visual acuities showed in Table 2 were estimated from the CSF cut-off frequencies determined in each CSF curve of the Fig. 4.

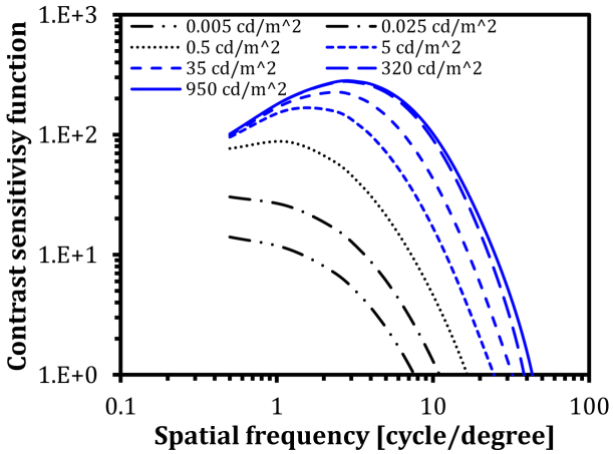

Fig. 4. CSFs determined for seven young subjects and seven luminance levels. Black curves correspond to mesopic levels, while blue curves at photopic levels.

In order to analyse the changes in the visual sensitivity resulting from the increment of lighting, the areas under the curves (AUC) of both the MTFs, NTFs, and CSFs were calculated. Fig 5. shows the contrast gain with the increment in retinal illuminance expressed as the NTFAUC. The values obtained for each lighting level studied yield an increasing response with a slope of 0.38 (open circles, R^2=0.90). The electrophysiological data measured by Purpura *et al.* in M cells (open squares), present a slope of 0.39 (R^2=0.86) [24] that strongly corresponds with our NTFAUC values for contrast gain, while the psychophysical data from Cao *et al.* for isolated cones (open triangles), with a slope of 0.29 (R^2=0.99) [25], has also a good agree. Note that the ordinate of each data set in Fig. 5 have been arbitrarily displaced for comparative purposes, avoiding the overlapping of the data. Also note that the axes in Fig. 5 are log-log, so the function fitted to each data set by least squares was a potential of the form $y = a.x^n$, where n corresponds to the slope of each line of the figure.

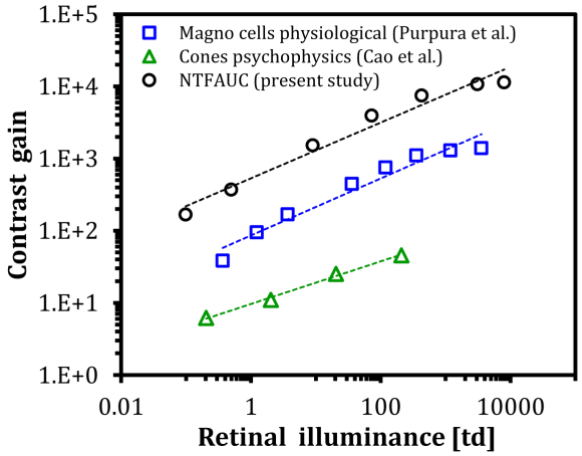

Fig. 5. Contrast gain as a function of the level of illumination estimated from the NTFAUC (open circles). Electrophysiological measurements of contrast gain of M cells (open squares) from Purpura *et al.* [24] and psychophysical measurements of contrast gain of isolated cones (open triangles) from Cao *et al.* [25] are added for comparison. To avoid the overlapping of the data, each data set was arbitrarily displaced in the ordinate.

The variations of the AUCs of MTF, NTF, and CSF as a function of illumination are showed in Fig. 6. In both NTF and CSF the AUCs grow with the same trend, the steepest slope in the mesopic range and then flattening towards the maximum measured luminance for the photopic range. The MTFAUC shows small variations for mesopic illumination levels and undergoes a sustained increase for photopic values (see the inner graph in Fig. 6) with a much more moderate overall AUC growth, going from a minimum of 3.9 to a maximum of 7.4.

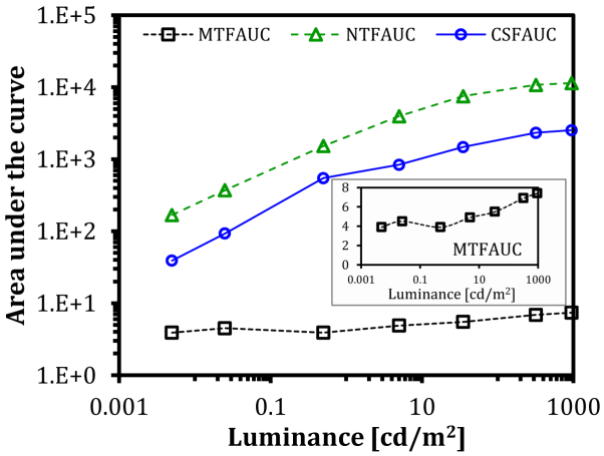

Fig. 6. Area under the curve values of the MTF (open squares), NTF (open triangles) and CSF (open circles) for the seven luminance levels considered. The inner graph shows the MTFAUC on a magnified scale.

Analysing the total growth of the MTF cut-off frequency, an increase by a factor of 1.8 was found while in the case of CSF the increment was by a factor of 5.4, implying an increment in the visual acuity (VA) that goes from 0.3 to 1.4 for all the luminance range studied (Table 2). Fig. 7 shows the variation of both cut-off frequencies as a function of luminance where can be observed that for the mesopic range the MTF cut-off frequencies are above to the CSF cut-off frequencies, however, in the photopic range both curves continue to grow and reach a coincident response.

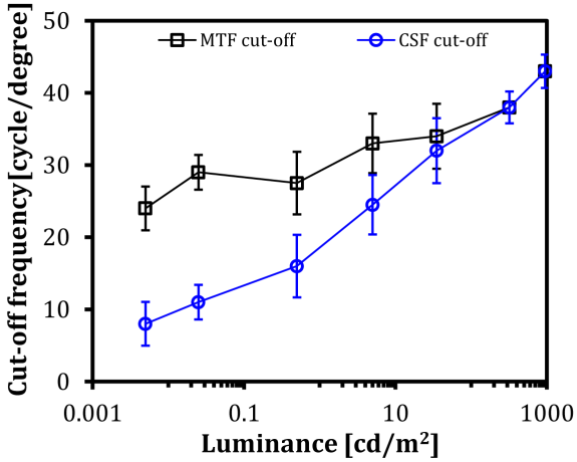

Fig. 7. Mean cut-off frequencies estimated for each luminance value. Open squares correspond to MTF cut-off and open circles correspond to CSF cut-off. Error bars represent ±1 SD.

4. Discussion and Conclusion

In this work we seek to analyse the contributions to spatial vision by the optics of the eye and the processing of visual information in the retina-brain pathway from a mixed strategy. First, we collected MTF data from a group of young subjects that allow us to characterize the optical response of the eye, while for the response of the neural tract we determined the neural transfer function NTF from the Barten's model [19]. To analyse the relative contributions of each part of the processing, we computed the area under curve for different adaptation conditions spanning much of the mesopic and photopic ranges. A priori, we know that the increase in the luminance of the adaptation field used to the determination of the MTF produces a monotonic reduction in the pupillary diameter, which in turn results in two phenomena: a reduction in ocular aberrations with the consequent increase in the visual quality that is expressed in the MTFAUC and an increase in retinal illuminance that produces a greater neural response expressed in the NTFAUC.

Because our analysis to obtain the CSF is based on the one hand on a curve calculated by a model (NTF) and on the other in a curve measured in the eye (MTF), the main limitation in our work comes from how these measures were performed. To obtain a representative measure of the visual system, the MTF should be polychromatic, while the MTF measured in our work is monochromatic. The wavelength chosen to perform

the measures corresponding to the NIR (785 nm) which has certain disadvantages that would be taken into account to then be able to interpret the results. On the one hand, the longer wavelengths are not absorbed by the retinal pigment epithelium and penetrate the deepest layers of the fundus of the eye, reaching the most vascularized layers such as choroids [31]. This brings a retro-diffusion that is present in the double-pass image, which if it is not taken into account, can be erroneously interpreted as ocular forward scattering which decreases both the cut-off frequency of the MTF and the area under the MTF curve, being both parameters used in our study. On the other hand, the MTF obtained for NIR is lower than that obtained for visible wavelengths, for example 555 nm [22]. When making measures in NIR, these factors must be taken into account when processing the images, in order to obtain an MTF that is as representative as possible of the visual system [3]. The only way to simultaneously measure the MTF and the pupil size adapted to an illuminated field is to use a non-visible wavelength, since otherwise the pupillary diameter is modified. This is an advantage that is used in the ophthalmological clinic using devices that allow measuring both the optical quality of the eye, aberrations, objective refraction, dynamics of the tear film, accommodation range, without the need to dilate the pupil.

The MTF of the human eye is mainly characterized as a passive low-pass filter presenting its best response to the lowest frequency, which cannot be greater than 1, and then decrease to a limit that is the maximum spatial frequency that can solve the optical system known as cut-off frequency. On the other hand, the NTF characterizes the stage of neural processing. In photopic levels, NTF behaves as an active pass-band filter with its greater response in an intermediate spatial frequency that decays towards low and high spatial frequencies. In addition, the visual signal is amplified by contrast gain mechanisms as can be seen in Fig. 5. In the mesopic range amplification also is presented but the shape of the curve corresponds to a low-pass filter (black curves in Fig. 4). The different characteristics of both kinds of filters (active-passive) avoid a direct comparison between their respective AUC because they are expressed in different scales. In order to know their relative contributions to the global response of the visual system, it is necessary to analyse each of the filters separately based on a variable such as luminance, which modifies both stages differently. In this kind of process (two consecutive filters) it should be taken into account that the efficiency of the first stage (MTF) largely determines the response of the second, for example, a low-quality retinal image cannot be corrected with an optimal neural function.

It is relevant to note that the analyse of the visual response for different lighting levels based on the calculation of the AUCs have a limitation: the global behavior is averaged in a number by integration for each lighting level avoiding to know the visual behavior in each specific range of spatial frequencies. Nevertheless, the proposed analysis of the cut-off frequencies allows us to know the particular behavior of the high spatial frequencies.

The MTF and NTF analysis depending on the luminance can be carried out taking into account its variations through the entire light range studied or considering different interest ranges. For example, within the mesopic there is a particular range of adaptation between 0.5 cd/m^2 and 3 cd/m^2 that corresponds to the typical lighting levels of public spaces and their roads, where people carry out various activities characterized by visual tasks of different complexities ranging from walking in a park, an activity with low visual demand, to driving a vehicle that requires greater resources from the visual system in a range where it does not present the best response. Therefore, in this range it could be relevant to know to what extent vision is affected by the factors that determine the visual quality of the eye, that is, aberrations and intraocular scattering. Thus, in the range of 0.5 cd/m^2 to 5 cd/m^2, an increase of 2.7 times in CSFAUC was found. This increase is largely explained by the increment of 2.6 times in NTFAUC and to a lesser extent by the increment of 1.3 times in MTFAUC. If the analysis is extended to the entire lighting range studied, an increase in lighting of 5.3 log units makes the MTFAUC almost double (1.9 times), while the NTFAUC increases 68 times and CSFAUC increases 65 times. However, the modest increment in the MTFAUC is associated with a reduction of 2.5 times of the aberrations expressed in terms of RMS (from 0.162 to 0.065) which represents an increase in the MTF cut-off frequency of almost double (from 24 to 43 cycles/degree).

Analysing the behaviour of MTFAUC and NTFAUC as a function of luminance we have found a significative result. At photopic levels above 100 cd/m^2 the neural response saturates while the optical response continues to increase. On the contrary, at the mesopic levels studied, an almost flat response of the MTF was observed, while the neural response presents a sustained growth. These results agree with those obtained by Hasting *et al.* from MTFs based on measurements of wavefront aberration from a population of normal healthy eyes using a Hartmann-Shack sensor and scaling the pupil sizes over a range of photopic and mesopic luminances [15]. Also, neural contrast sensitivity data were obtained from global contrast

sensitivity computed with the model of Rovamo *et al.* [27], which in turn was scaled to obtain functions at different levels of retinal illuminance between 0.9 and 9000 td [28]. To assess the optical and neural contributions to contrast sensitivity, they defined an index based on an *ad hoc* Strehl ratio that was calculated with the integrals of the proposed functions, that is, even when the procedures are different to our proposal, the operations of integrating of the contributions of each stage of the visual process is equivalent to our simplest operation of calculating the AUCs. Besides, the Rovamo *et al.* model is fully compatible with the Barten's model comprising a low-pass filtering accounting the MTF and similar neural process [19,27]. These results and the tools used to obtain them raise the possibility of extending these studies by incorporating the age variable through MTF models and also open up the possibility of analysing the relative contributions of the different spatial frequency ranges that the visual system processes from the different neural mechanisms that operate in it. The correspondence between the slopes of contrast gain determined with different approaches presented in Fig. 5 shows that the NTF model used describes adequately the neural response across the range of luminance used in this study.

The high MTF cut-off frequencies values above to the CSF cut-off frequencies in the mesopic range which are presented in the Fig. 7 suggest the optical response is limited by the neural processing and does not reach to effectively contribute to achieving the best visual response. In the photopic, the neural response increases enough so that account for the spatial resolution provides by the optic response. In other words, although NTF explains much of the CSF improvement when illumination increases, the contribution of the optical response reaches an optimal level of spatial resolution that is follows by the neural processing only at the photopic level achieving the optimal spatial resolution of the visual system.

There are some works in the literature that propose an analysis of visual quality and the influence of optical and neural factors on the visual system [15,19,27-29]. Some of these works are based on analysis of models under different conditions (luminance, age, pupil size, etc.), while others use a combination of measures with models. One of the main contributions of present study is to have obtained similar and compatible results with those found by other authors, using different methods. In this sense, all the results found were expected, however, we could verify that a reliable visual quality parameter can be obtained from the MTF estimated through the double-pass method combined to an NTF model proposed in the literature [19]. As far as we know, our work is one of the few in which pupil size, test luminance, MTF of the eye and aberrations are simultaneously measured. In the literature there are works in which the luminance of the test is fixed and, with dilated pupil by drops, different artificial pupils are set to make the measures [26]. Other works set a single artificial pupil size (prior dilation of the natural pupil) and vary the luminance of the target [30]. With any of the two methods, a variation in retinal illuminance can be reached, which is then applied to neural contrast sensitivity models. However, these values are not representative of what happens in normal vision conditions, where there is an interaction between the luminance of the visual scene and the dynamics of the pupil. In this sense, we believe that our work is relevant since the proposed visual parameter is based on the MTF of the measured eye under a certain illumination condition, and on a validated model of neural contrast sensitivity calculated with the data from the same conditions of measure of the MTF (age, luminance, pupil size, etc.). The other relevant contribution consists in considering the intraocular scattering in the MTF measured which is not taken into account by Hastings *et al.* because they used a different method to determine the MTF [15]. The consideration of this variable is very important when the age is incorporated in the study. Our analysis was based on the FSI which presented, for young subjects, a very low variation as a function of the luminance and pupil diameter showing its robustness and independence of the aberrations in the same way that was found in previous works so it is expected that in measurements carried out on older adults FSI will increase significantly [16,23].

Acknowledgements

This work was supported by Consejo Nacional de Investigaciones Científica y Técnicas (CONICET, grant number PUE 0114, and grant number PIP 2721), Consejo de Investigaciones de la Universidad Nacional de Tucumán (CIUNT, grant number PIUNT E646). The authors report no conflicts of interest and have no proprietary interest in any of the materials mentioned in this article.

